

Optical self-phase modulation using a new photonic crystal coupled-cavity waveguide

SHAHRAM BAHADORI-HAGHIGHI, RAHIM GHAYOUR*

Department of Electrical and Computer Engineering, Shiraz University, Shiraz, Iran

*Corresponding author: rghayour@shirazu.ac.ir

In this paper, self-phase modulation of an optical pulse using a new photonic crystal coupled-cavity waveguide is simulated and analyzed. The structure of the new coupled-cavity waveguide is introduced and its advantage over the previous type of coupled-cavity waveguide is discussed. In order to obtain a high group index over a large bandwidth and benefit from the slow light phenomenon, the group index and group velocity dispersion parameter curves of the guided mode are calculated. Finally, the transient simulation of the structure is performed using a finite-difference time-domain method. The calculated required length of the coupled-cavity waveguide for a maximum phase shift of π is about 31 μm . Spectral broadening of the optical pulse as a result of self-phase modulation is also presented and discussed.

Keywords: photonic crystal, slow light, coupled-cavity waveguide, self-phase modulation.

1. Introduction

All optical processing has been of particular interest for optical communication and computing systems. Different types of all optical devices have already been proposed and implemented to achieve large bandwidth operations in optical systems [1–5]. All optical devices are based on weak optical nonlinear effects. Therefore, such devices need high operational powers and large interaction lengths. Photonic crystal (PhC) is a good means to overcome such limitations. PhC is a class of artificial optical material in which the refractive index changes periodically. Light beams within a specific range of wavelengths and with specific polarizations are prohibited from propagation inside a PhC. This specific range of wavelengths is called photonic bandgap.

Slow light phenomenon as an approach to enhance light-matter interactions causes significant size reduction of nonlinear optical devices. Researches on this phenomenon have been pursued in different media by many authors [6–8]. A PhC waveguide is a device in which slow light has already been observed [9, 10]. The slope of dispersion curves of the guided modes in PhC waveguides tends to decrease at the edge of

the Brillouin zone and therefore the slow light condition in this regime is achieved. However, high group velocity dispersion (GVD) in this region limits the available bandwidth and eliminates the advantages associated with the slow light phenomenon. Nevertheless, in PhC waveguides with their geometrical flexibility, it is possible to create slow modes in regions away from the edge of the Brillouin zone [11–13].

Coupled-cavity waveguides (CCWs) based on PhCs have already been investigated [14–17]. In a CCW which consists of a chain of cavities to create a line defect, light propagates down the waveguide via tunneling from one cavity to its neighboring cavity. This process creates propagation of slow modes in such waveguides.

In this paper we first review the structure of the old PhC-CCW and illustrate its limitation. Then, the schematic of a new PhC-CCW is introduced and its advantage over the previous type of CCW is discussed. In Section 3, the group index and the GVD of the appropriate guided mode of the new CCW is investigated. Next, according to the results, the geometry of the waveguide is chosen so that a high group index over a large bandwidth with low GVD is obtained. Finally in Section 4, self-phase modulation (SPM) of an optical pulse by use of the designed slow light CCW as short as about $31\ \mu\text{m}$ is observed. Such structure could be useful in the context of nonlinear optics including fast intensity-based switches and soliton-based transmission systems.

2. Analysis of photonic crystal coupled-cavity waveguides

The structure of the old type PhC-CCW originally proposed by YARIV *et al.* [18] and followed further by SOLJAČIĆ *et al.* [16, 17], is shown in Fig. 1a. The structure is a periodic array of point defects which are mutually spaced by Λ_1 in a square lattice rod-type PhC. An optical beam can propagate down the waveguide through tunneling from

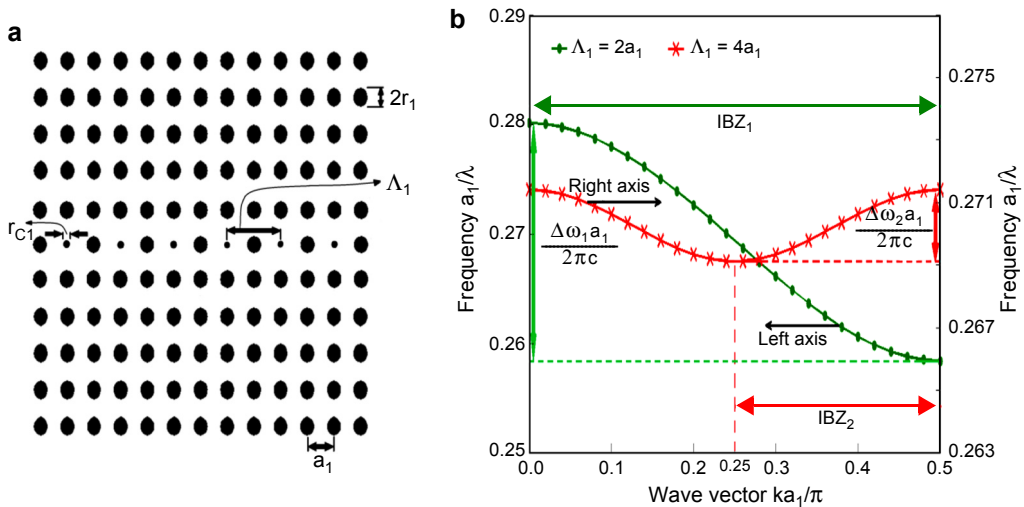


Fig. 1. The schematic of the old type of PhC-CCW (a). Dispersion curves of the guided mode for two cases of $\Lambda_1 = 2a_1$ and $\Lambda_1 = 4a_1$ (b). (Color online.)

one cavity to its neighboring cavities. This process of propagation makes the group velocity v_g of the guided mode slow. Increasing the physical distance between the cavities Λ_1 is the only approach to make the group velocity of the guided mode slower. The dispersion curve of the guided mode for two cases of $\Lambda_1 = 2a_1$ and $\Lambda_1 = 4a_1$ (a_1 is the lattice constant) is depicted in Fig. 1b. The refractive index of dielectric rods embedded in air background is assumed to be 3.5. The radii of dielectric rods and cavity rods (reduced-radius rods in the cavities) are taken to be $r_1 = 0.25a_1$ and $r_{C1} = 0.15a_1$, respectively. As it is seen, the size of the irreducible Brillouin zone (IBZ) for the case of $\Lambda_1 = 2a_1$ is twice that of the case of $\Lambda_1 = 4a_1$ ($IBZ_1 = 2IBZ_2$). Therefore, as it is shown in Fig. 1b, the dispersion curve covers narrower range of frequencies when $\Lambda_1 = 4a_1$ (i.e. $\Delta\omega_1 a_1 / 2\pi c > \Delta\omega_2 a_1 / 2\pi c$). Consequently, decreasing the group velocity by increasing the periodicity of the PhC-CCW lowers the size of the IBZ which, in turn, reduces the accessible bandwidth.

The schematic of the new PhC-CCW is shown in Fig. 2a. The structure is based on a square lattice PhC which consists of dielectric rods with refractive index of 3.5 embedded in air background. The radius of a row of dielectric rods is reduced from $r = 0.25a$ (a is the lattice constant) to $r_r = 0.15a$. The cavity rods are made by increasing the radius of every third rod ($\Lambda = 3a$) in the two rows adjacent to the reduced-radius rods. The radii of the cavity rods are indicated by r_C in Fig. 2a. The refractive indices

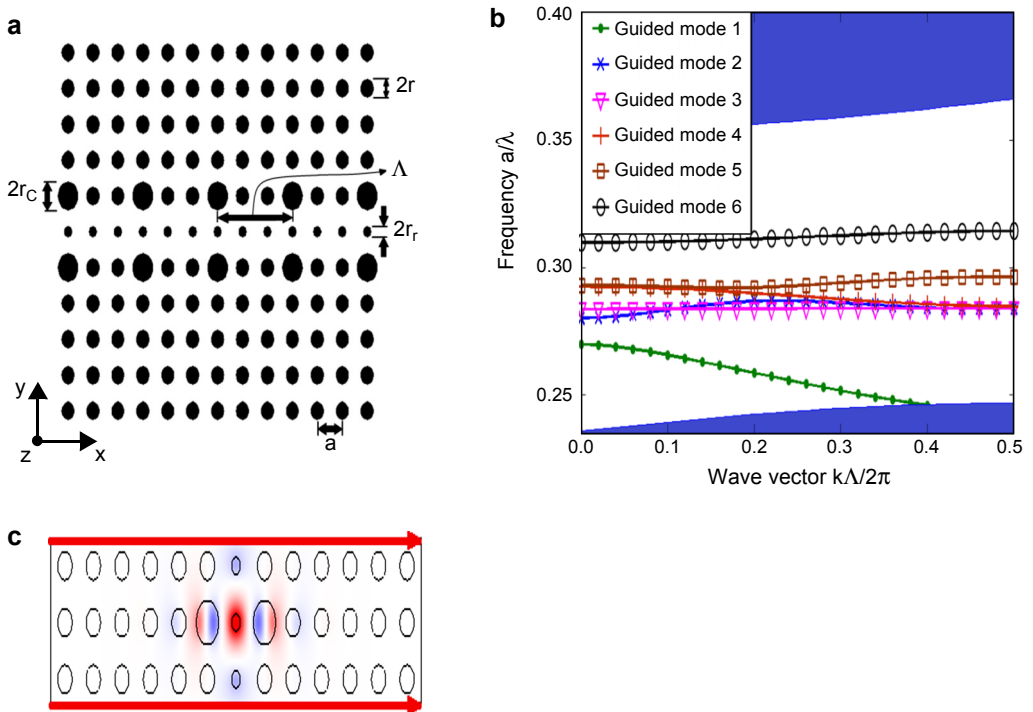


Fig. 2. The schematic of the new PhC-CCW (a) and its corresponding band structure (b). The electric field profile inside a super-cell of the structure (c). (Color online.)

of the rods are taken the same as that of the CCW shown in Fig. 1a. The band structure of the new PhC-CCW and its six guided modes for TM polarization are shown in Fig. 2b. This diagram is calculated using the finite-element method (FEM) by COMSOL Multiphysics. The computational (unit) cell is shown in Fig. 2c, where the eigenfrequency analysis tool of the software is used to find the guided modes. As it is clear, if the unit cell is repeated over the boundaries (arrows in Fig. 2c), the whole structure of the waveguide will be constructed. Hence, the periodic boundary conditions are applied to the red boundaries in Fig. 2c. We also use the normal predefined mesh size of the software which generates 17568 elements in our computational cell.

As it is shown in Fig. 2b, guided modes 1 and 6 do not overlap with other modes. Hence, intermodal dispersion can be avoided by choosing one of these two modes as the operating mode. Moreover, as guided mode 6 has a lower group velocity than that of guided mode 1, therefore, we choose guided mode 6 as the appropriate operating mode to benefit from the advantages of slow light. The electric field distribution of this guided mode in a super-cell of the structure is depicted in Fig. 2c.

The new PhC-CCW provides another approach to obtain slower modes without reduction of the IBZ to avoid severely limited bandwidth. In this way, the slope of the dispersion curve of the guided mode could be changed by modifying the radius of the cavity rods r_C as illustrated in Fig. 3. It is seen that the slope of the dispersion curve of guided mode 6 is reduced by decreasing the radius of the cavity rods and therefore the group velocity of the guided mode decreases. Hence, changing the radius of the cavity rods can be a useful approach to adjust the group velocity to an appropriate value.

At the end of this section, it should be noted that the new PhC-CCW shown in Fig. 2a is a 2D rod-type PhC waveguide in which the rods are infinite along the z -direction. Such a 2D structure has been taken for simplicity and also to compare it with the rod-type PhC-CCW investigated by SOLJAČIĆ *et al.* [16, 17], shown in Fig. 1a.

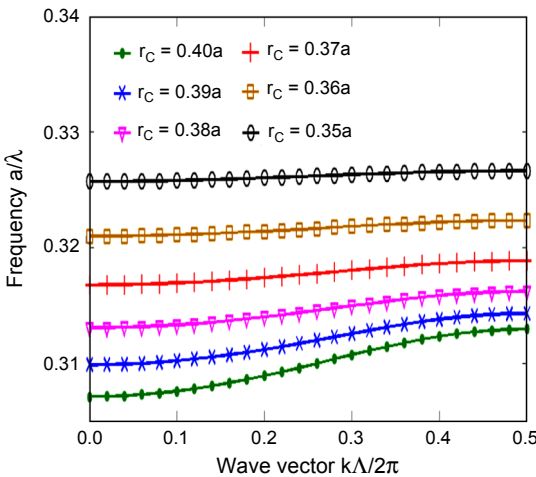


Fig. 3. Dispersion curve of guided mode 6 for different radii of the cavity rods r_C . (Color online.)

However, from a practical point of view, the waveguides must have a finite thickness along the z -direction. In such a case, hole-type waveguides which consist of holes in a dielectric background, are preferable. Hole-type waveguides can reduce out-of-plane losses by confining optical beam in the z -direction through total internal reflection. The so-called propagating optical beams are transverse electric (TE) modes which are located below the light line in the corresponding band structure. However, the main feature of the new PhC-CCW shown in Fig. 2a is the kind of cavities which are constructed in such a way to be modified locally. Clearly, as a subject of a subsequent investigation, one can preserve this main feature and apply it to design a hole-type PhC-CCW to take its advantage (which was mentioned earlier in this section).

3. Guided mode analysis

In order to determine the appropriate geometric parameters of the structure for transient simulation, guided mode analysis is done. The most important issue in slow light devices is the value of group index (*i.e.*, $n_g = c/v_g$). The calculated group index curves corresponding to the guided modes of Fig. 3 are plotted vs. normalized frequency a/λ in Fig. 4a. As it is seen, all the n_g curves are in U-shape. It means that as the frequency increases, first the value of n_g decreases, then it stays nearly constant over a specific bandwidth and finally it starts to increase at the edge of the IBZ. Figure 4a illustrates that by decreasing the radius of the cavity rods, the value of n_g in the constant region increases and the guided mode slows down more. Furthermore, by decreasing the radius of the cavity rods, the bandwidth over which n_g remains approximately constant, decreases. Therefore, there exists an intrinsic compromise between the value of the group index and the bandwidth.

It seems that the best choice is to create the largest value of group index for enhancing optical nonlinear effects. However, another important issue in the context of

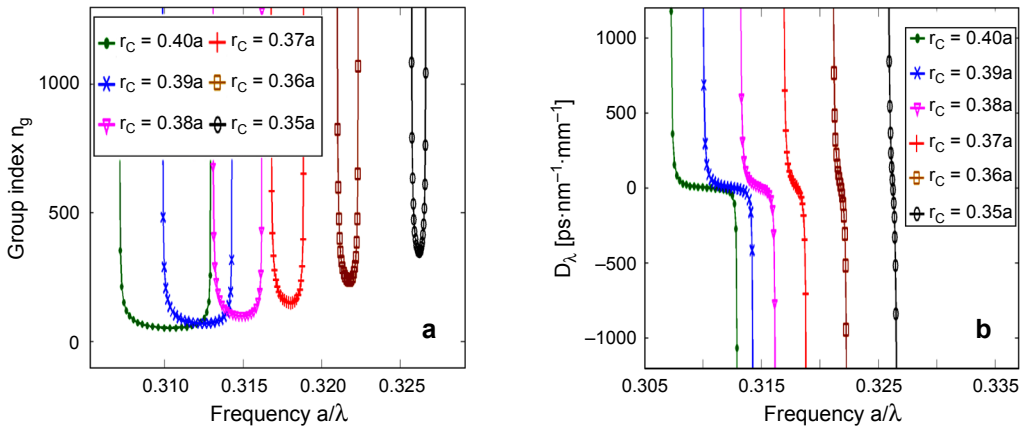


Fig. 4. Group index n_g (a) and GVD parameter D_λ (b) of guided mode 6 for different radii of the cavity rods r_C . (Color online.)

slow light devices is the GVD. Due to temporal broadening of optical pulses which limits the bit rate in optical transmission systems, large GVD is generally undesirable. Furthermore, as another consequence of temporal broadening, the peak intensity of pulses is reduced and it removes the enhancement of nonlinear effects expected from the slow light pulse compression [19].

The GVD parameter D_λ of a guided mode is obtained as follows [20]:

$$D_\lambda = -\frac{2\pi c}{\lambda^2} \frac{\partial^2 k}{\partial \omega^2} \quad (1)$$

where c is the light speed in vacuum and k is the wave vector. The calculated GVD parameter of guided mode 6 for different radii of cavity rods is shown in Fig. 4b. As it is shown, for larger values of r_C there is a bandwidth within which the GVD parameter is nearly zero. This condition corresponds to the constant n_g region of Fig. 4a. As the radius of the cavity rods decreases, the value of the group index increases and the corresponding bandwidth of low GVD region is reduced consequently.

According to Figs. 4a and 4b, in order to have a large group index and at the same time low GVD, the radius of $r_C = 0.39a$ is selected for the cavity rods. In this case, the value of group index in the low GVD region is $n_g \cong 70$ that is large enough to take advantage of the slow light phenomenon. We select $a/\lambda \cong 0.312$ as the operating point of guided mode 6. For the operating wavelength of $\lambda = 1.55 \mu\text{m}$ the lattice constant is obtained as $a \cong 0.483 \mu\text{m}$.

4. Transient simulation and discussion

In this section, SPM of an optical pulse is performed so that a phase shift of π is acquired at the peak intensity of the pulse. First, we assume that only the reduced-radius rods in the CCW structure of Fig. 2a have Kerr nonlinearity similar to the previous work [21]. The change in the refractive index of a nonlinear material due to the optical Kerr effect is obtained as follows [22]:

$$\Delta n = \frac{3\chi^{(3)}}{4n_0^2 \epsilon_0 c} I_0 \quad (2)$$

where $\chi^{(3)}$ is the third-order nonlinear susceptibility, n_0 is the linear refractive index, ϵ_0 is the permittivity of free space and I_0 is the intensity of the optical beam.

The refractive index of dielectric rods is 3.5 and $\chi^{(3)}$ for the reduced-radius rods is $4.4 \times 10^{-19} \text{ m}^2/\text{V}^2$ that is the third-order nonlinear susceptibility of AlGaAs. Therefore, according to Eq. (2), the required peak intensity of the optical pulse for a refractive index change of $\Delta n = 0.01$ will be $I_0 \cong 98.6 \text{ GW}/\text{cm}^2$ that is a very large value.

Now, the transient simulation of the CCW shown in Fig. 2a is done using 2-D finite-difference time-domain (FDTD) method to demonstrate SPM. Numerical resolution of the simulation is set to $45 \times 45 \text{ pixel}/\mu\text{m}^2$ and a Gaussian pulse at a center

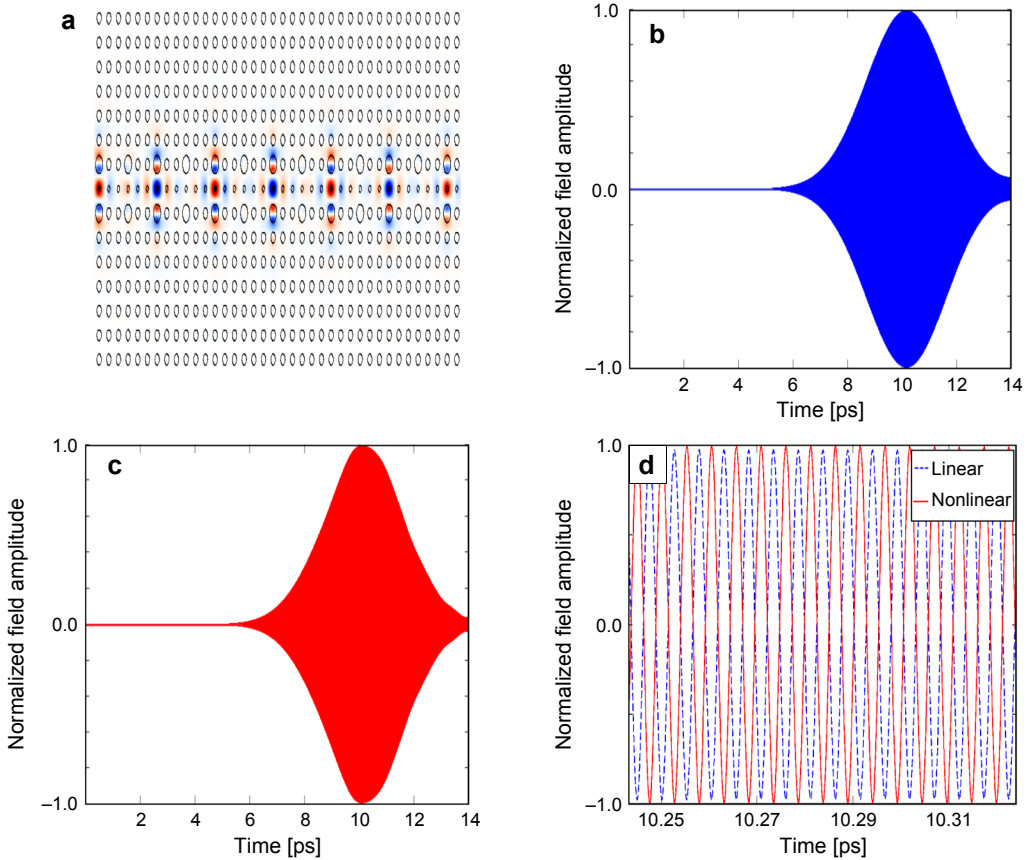


Fig. 5. Snapshot of the optical beam propagating along the line defect of the new CCW (a). The normalized electric field amplitude of the optical pulse at the output for the linear (b) and nonlinear (c) cases. The normalized electric field amplitudes at the peak of the pulse for the linear and nonlinear cases (d). (Color online.)

wavelength of $1.55 \mu\text{m}$ is launched. The snapshot of the light beam propagating down the PhC-CCW is shown in Fig. 5a. In order to show the effects of SPM on the optical pulse, linear and nonlinear simulations of the structure are performed. According to the transient simulation and as a result of the slow light spatial pulse compression, the required input peak intensity of the pulse is just $I \cong 0.015I_0 \cong 1.48 \text{ GW/cm}^2$. As a matter of fact, the slow light condition provided by the slow operating mode causes the input pulse to be compressed and the peak intensity of the pulse increases from $I \cong 1.48 \text{ GW/cm}^2$ to $I_0 \cong 98.6 \text{ GW/cm}^2$. On the other side, as it is mentioned above, the peak intensity of the pulse causes a refractive index change of $\Delta n = 0.01$ in the reduced-radius rods having nonlinear Kerr property. Consequently, a relative phase shift of $\Delta\varphi = \pi$ with respect to the linear case is obtained at a short length of about $31 \mu\text{m}$ away from the input source. The electric field amplitudes of the optical pulse at the output for the linear and nonlinear cases are shown in Figs. 5b and 5c. In order to

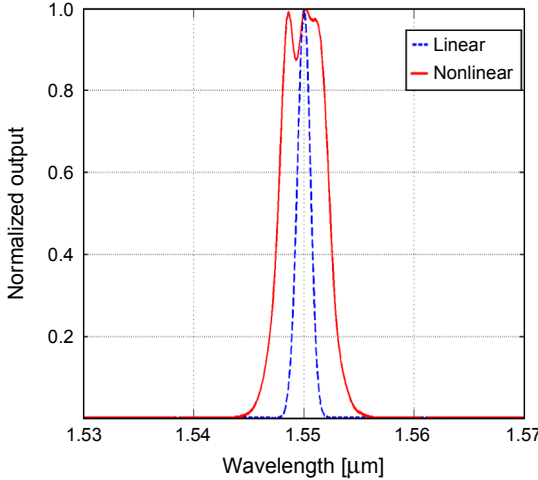


Fig. 6. Output spectra of the optical pulse at the output of the CCW for the linear and nonlinear cases.

illustrate the induced phase shift of π , the electric field amplitude at the peak of the pulse in the nonlinear case together with the one in the linear case is depicted in Fig. 5d. Indeed, a propagation constant perturbation Δk is induced when the refractive index of the reduced-radius rods changes by the intensity of the optical pulse in the nonlinear case. This in turn causes the peak optical field of the input pulse to accumulate π more phase shift in the nonlinear case with respect to the linear one.

At the end of this section, the spectrum of the optical pulse at the output of the waveguide is investigated. The spectra of the optical pulse for the linear and nonlinear cases are shown in Fig. 6. As it is seen, the spectrum of the pulse in the nonlinear case is broadened. In other words, SPM manifests itself as the generation of the new frequencies across the optical pulse as described by $\partial\omega(t) = -(\partial/\partial t)\Delta\varphi(t)$. According to this relation, on the front end of the pulse, red-shifted frequencies are generated by SPM as the phase shift is increasing with the intensity of the pulse. On the tail of the pulse, blue-shifted frequencies emerge from SPM as the phase shift is decreasing. The so-called spectral broadening of an optical pulse as a result of SPM is very useful in many applications. It can be used to produce ultra short pulses at high repetition rates or as an approach for dispersion compensation to create optical solitons.

5. Conclusions

In summary, we presented that the new PhC-CCW can provide another approach to achieve slow modes. Such an approach does not decrease the IBZ and therefore the reduction of the accessible bandwidth will not be as much as the one caused by the approach used in the old PhC-CCW. Using guided mode analysis, we demonstrated that as the radius of the cavity rods in the new PhC-CCW is reduced, the group index increases and at the same time the corresponding bandwidth of the low GVD region decreases. The radius of the cavity rods was selected to have $n_g \cong 70$ and obtain

an acceptable bandwidth over the low GVD region. Finally, SPM of a Gaussian pulse at the center wavelength of $1.55 \mu\text{m}$ was performed and the results were presented. The required length for the maximum phase shift of π was obtained as short as $31 \mu\text{m}$. Moreover, as one of the great results of the slow light phenomenon, the needed intensity at the peak of the input pulse for $\Delta n_{\text{max}} = 0.01$ in the reduced-radius rods, decreased from $I_0 \cong 98.6 \text{ GW/cm}^2$ to $I \cong 0.015I_0 \cong 1.48 \text{ GW/cm}^2$. The spectral broadening of the optical pulse as another result of SPM that could be useful in many practical applications was also illustrated.

References

- [1] YULAN FU, XIAOYONG HU, QIHUANG GONG, *Silicon photonic crystal all-optical logic gates*, Physics Letters A **377**(3–4), 2013, pp. 329–333.
- [2] WEN-PIAO LIN, YU-FANG HSU, HAN-LUNG KUO, *Design of optical NOR logic gates using two dimension photonic crystals*, American Journal of Modern Physics **2**(3), 2013, pp. 144–147.
- [3] ARKHIPKIN V.G., MYSLIVETS S.A., *All-optical switching in a photonic crystal with a defect containing an N-type four-level atomic system*, Physical Review A **86**, 2012, article 063816.
- [4] NOZAKI K., TANABE T., SHINYA A., MATSUSO S., SATO T., TANIYAMA H., NOTOMI M., *Sub-femtojoule all-optical switching using a photonic-crystal nanocavity*, Nature Photonics **4**(7), 2010, pp. 477–483.
- [5] HUA LU, XUEMING LIU, LEIRAN WANG, YONGKANG GONG, DONG MAO, *Ultrafast all-optical switching in nanoplasmonic waveguide with Kerr nonlinear resonator*, Optics Express **19**(4), 2011, pp. 2910–2915.
- [6] LUKIN M.D., IMAMOGLU A., *Controlling photons using electromagnetically induced transparency*, Nature **413**(6853), 2001, pp. 273–276.
- [7] BIGELOW M.S., LEPESHKIN N.N., BOYD R.W., *Observation of ultraslow light propagation in a ruby crystal at room temperature*, Physical Review Letters **90**, 2003, article 113903.
- [8] DAQUAN YANG, XUEYING WANG, HUIPING TIAN, YUEFENG JI, *Electro-optic modulation property of slow light in coupled photonic crystal resonator arrays*, Optica Applicata **41**(3), 2011, pp. 753–763.
- [9] KRAUSS T.F., *Slow light in photonic crystal waveguides*, Journal of Physics D: Applied Physics **40**(9), 2007, pp. 2666–2670.
- [10] BABA T., *Slow light in photonic crystals*, Nature Photonics **2**(8), 2008, pp. 465–473.
- [11] JUNTAO LI, WHITE T.P., O'FAOLAIN L., GOMEZ-IGLESIAS A., KRAUSS T.F., *Systematic design of flat band slow light in photonic crystal waveguides*, Optics Express **16**(9), 2008, pp. 6227–6232.
- [12] KUBO S., MORI D., BABA T., *Low-group-velocity and low-dispersion slow light in silicon photonic crystal waveguides*, Optics Letters **32**(20), 2007, pp. 2981–2983.
- [13] EBNALI-HEIDARI M., GRILLET C., MONAT C., EGGLETON B.J., *Dispersion engineering of slow light photonic crystal waveguides using microfluidic infiltration*, Optics Express **17**(3), 2009, pp. 1628–1635.
- [14] MATSUDA N., KATO T., HARADA K., TAKESUE H., KURAMOCHI E., TANIYAMA H., NOTOMI M., *Slow light enhanced optical nonlinearity in a silicon photonic crystal coupled-resonator optical waveguide*, Optics Express **19**(21), 2011, pp. 19861–19874.
- [15] ÜSTÜN K., KURT H., *Ultra slow light achievement in photonic crystals by merging coupled cavities with waveguides*, Optics Express **18**(20), 2010, pp. 21155–21161.
- [16] SOLJAČIĆ M., JOANNOPOULOS J.D., FAN S., IBANESCU M., IPPEN E., JOANNOPOULOS J.D., *Photonic-crystal slow-light enhancement of nonlinear phase sensitivity*, Journal of the Optical Society of America B **19**(9), 2002, pp. 2052–2059.
- [17] SOLJAČIĆ M., JOANNOPOULOS J.D., *Enhancement of nonlinear effects using photonic crystals*, Nature Materials **3**(4), 2004, pp. 211–219.
- [18] YARIV A., YONG XU, LEE R.K., SCHERER A., *Coupled-resonator optical waveguide: a proposal and analysis*, Optics Letters **24**(11), 1999, pp. 711–713.

- [19] MONAT C., CORCORAN B., PUDO D., EBNAI-HEIDARI M., GRILLET C., PELUSI M.D., MOSS D.J., EGGLETON B.J., WHITE T.P., O'FAOLAIN L., KRAUSS T.F., *Slow light enhanced nonlinear optics in silicon photonic crystal waveguides*, IEEE Journal of Selected Topics in Quantum Electronics **16**(1), 2010, pp. 344–356.
- [20] RAN HAO, CASSAN E., KURT H., LE ROUX X., MARRIS-MORINI D., VIVIEN L., HUAMING WU, ZHIPING ZHOU, XINLIANG ZHANG, *Novel slow light waveguide with controllable delay-bandwidth product and ultra-low dispersion*, Optics Express **18**(6), 2010, pp. 5942–5950.
- [21] FUJISAWA T., KOSHIBA M., *Finite-element modeling of nonlinear Mach–Zehnder interferometers based on photonic-crystal waveguides for all-optical signal processing*, Journal of Lightwave Technology **24**(1), 2006, pp. 617–623.
- [22] BOYD R.W., *Nonlinear Optics*, 2nd Ed., Academic Press, New York, 2003.

*Received September 16, 2013
in revised form November 30, 2013*